NASA TECHNICAL TRANSLATION

NASA TT F-11,510

NASA TT F-11,510

RECENT DEVELOPMENTS IN WIND-TUNNEL MEASUREMENTS OF AERODYNAMIC DERIVATIVES

M. Scherer and J. Lopez

Translation of "Progres Realises dans les Techniques de Mesure des Derivees Aerodynamiques en Soufflerie Methode d'Oscillations Forcees"
Office National d'Etudes et de Recherches Aerospatiales, TP 389, 1967, 32 p.

NATIONAL AERONAUTICS AND SPACE ADMINISTRATION
WASHINGTON, D.C. 20546 MARCH 1968

TABLE OF CONTENTS

NASA TT F-11,510

RECENT DEVELOPMENTS IN WIND-TUNNEL MEASUREMENTS OF AERODYNAMIC DERIVATIVES

M.Scherer and J.Lopez

ABSTRACT. Some of the most important unsteady-testing devices used in wind-tunnels are presented. These devices give the complete set of derivatives, the knowledge of which is necessary to the study of flight mechanics of planes or missiles. The tests can be carried out in continuous or in intermittent wind-tunnels. Sting dynamometers and micro-accelerometers equipped with silicium strain-gages are now employed. An example is given for comparison of the wind-tunnel measurements; it deals with the measurement in flight and in wind-tunnel of the STOL-Breguet 941 in landing configuration.

1. Introduction

The object of this publication is to offer a glance at the progress made at /3* l'O.N.E.R.A. in the measurement of aerodynamic derivatives by the method of forced oscillations since the communication made in Brussels in 1961 [1].

A preliminary remark is necessary: unsteady derivatives represent only one aspect of the information required solely for studies of flight quality. As a result, their determination in a wind-tunnel will be of interest to designers only if they are obtained easily and rapidly. On the other hand, however, a relatively broad tolerance in terms of precision will be admitted.

It is with this in mind that the O.N.E.R.A. measurement installations were created and developed; some operate with forced oscillations and others operate with free oscillations [2].

The disclosure to follow will deal strictly with the method of forced oscillations.

The principles of these methods are well known and will be brought up only to refresh the reader's memory. The considerable progress achieved in measurement techniques in recent years will be especially stressed.

The principal installations of this type now in service at O.N.E.R.A. will be presented.

Some cross-checking against flight measurement will give an idea of the validity of the wind-tunnel results.

---

* Numbers in the margin indicate pagination in the foreign text.

2. Notations

The notations used are in conformity with the French standards X 02-105.

Special notations are presented:

- in the table in Plate 2, where the expressions for the dimensionless coefficients of the aerodynamic derivatives are given.

- in the figures in Plate 3, where the fixed reference axes and the reference axes related to the mock-up are given, as well as the symbols for the angles, the components of the resulting moment (L_1, M_1, N_1) and for the angular velocity (p_1, q_1, r_1) on the axes bound to the mock-up (Figure 1).

3. Description of Principal Arrangements and Methods /4

3.1. Jetstream Mounting

The mock-up is attached to the end of a dynamometric sting similar to those used for stationary measurements.

Strain gages are fastened to the forward part of the sting and assembled in combination by groups of four, each of which is a moment dynamometer.

Five dynamometers are thereby formed which yield the projected moments according to two systems of axes, specifically:

$$0_1^1 \quad x_1 \quad y_1^1 \quad z_1^1 \quad , \quad 0_1^2 \quad x_1 \quad y_1^2 \quad z_1^2 \quad ,$$

having in common the axis $0_1^1\ 0_1^2\ x_1$ and reduced one from the other by translation of $0_1^1\ 0_1^2$ along the x_1 axis (Figure 2).

The subscript 1 indicates that the system of axes is connected to the sting and therefore to the mock-up, and the superscript is used to differentiate them.

The component parallel to the sting is not measured. The names and symbols of the five components are indicated in the table below.

Angular elongation of the movement of the mock-up during oscillation is /5
measured by a detector equipped with strain gages similar to those of the dynomometers (Figure 3). This detector is indicated by D in Figure 5.

3.2 Setting into Motion

Constant low-amplitude oscillations ($\sim 2°$) with constant frequency

($1 < f \leq 20$ Hz) are fed the mock-up and the sting successively around the three axes either blended with or parallel to the axes defined above, by a simple mechanical device.

TABLE

Measured	Symbol	Reduction axis of moment
Roll	L_1	$0_1^1 \quad x_1$
Yaw	N_1^1 N_1^2	$0_1^1 \quad z_1^1$ $0_1^2 \quad z_1^2$
Pitch	M_1^1 M_1^2	$0_1^1 \quad y_1^1$ $0_1^1 \quad y_1^2$

The roll motion around the sting axis is generally easily obtained.

In contrast, even in Modane's large supersonic wind-tunnels, the size of the mock-ups presently being used does not in practice permit the use of oscillations around an axis passing through the representative point for the center of gravity in the aircraft or engine undergoing tests.

For measurements in supersonic or transonic wind-tunnels, this reason has resulted in the fixing of the pitch or yaw oscillation axes downstream from the mock-up.

Allowance has been made in computations for the lack of concurrence between the oscillation and measurement axes [§ 3.3].

3.3 Measurement Methods

The indications for the dynamometer and position detector as a function of time are treated by harmonic analysis limited to the frequency of the motion imposed.

This method of operation has the advantage of automatically eliminating from the measurement results the parasite responses introduced by the continuous components and harmonic resulting from noises of the wind-tunnel and the mounting.

This limitation is sufficient if the responses are linear, a frequent case in practice. Two processes are used for the application of the method:

1) The first, developed and perfected 15 years ago, applies to continuous wind-tunnels. In this process, the wind-tunnel data are obtained by direct reading during the tests.

It consists of feeding the gage bridges by a sinusoidal current with constant intensity and a frequency identical to that of the motion imposed (Plate 5).

The phase for this current is repeatedly adjusted, first in coincidence with the motion and then squared. Constant-current galvanometers, the same as those used for stationary measurement and plugged into the measurement diagonals for the bridges yield respectively: /6

- After the first adjustment, the amplitudes for the moment components $R(M_1)$ etc... in phase with the motion and the amplitude of the latter $R(\Theta_1)$ [or $R(\psi_1)$ or $R(\Phi_1)$].

- Following the second adjustment, the components of the moment $J(M_1)$ etc... in quadrature with the motion. In this case the galvanometer plugged into the position detector must show a zero indication [$J(\theta) = 0$], according to the definition of the square.

It is precisely in acting on the phase converter so as to cancel the galvanometer reading that the adjustment is first achieved then maintained throughout the measurement.

2) In the second process, the gages are fed a continuous current and the responses fixed in the bridge measurement diagonals are treated by harmonic analysis (Plate 6).

This may be done in two ways:

1 - Immediately during the tests by an analogical means.

2 - Delayed and using a magnetic recorder; in this case the harmonic analysis may be carried out with the same precision by either a numerical or analog process.

The advantage of delayed clearing is that it permits measurement of forced oscillations in intermittent wind-tunnels where the useful duration of the flow is on the order of one second.

Tests in the fine adjustment of this measurement chain were carried out in the O.N.E.R.A. intermittent wind-tunnel at Chalais-Meudon equipped with a Mach 10 tube through measurement of the pitch derivatives of a mock-up of a blunt cone [3].

This setup is presently being adapted to industrial measurement.

In each case, the data of harmonic analysis, direct or delayed, are then transformed into the dimensionless coefficients indicated in Plate 2.

These calculations, performed automatically, introduce various corrections (energy forces, non-measured support deformations, non-concurrence of oscillation and measurement axes).

The calculation programs on the IBM 704 will be the subject of another publication.

4. Progress Achieved /7

The progress which has been achieved in the last four years has had a bearing on both improving the measurement chains and the development of the mounting installations.

4.1 Measurement and Control Channels

Electronic Equipment.

Various types of equipment designed almost integrally with commercially mass-produced transistorized sets have been put into service:

- controlled feed of the electric motors which perform the oscillation motions.

The rotation speed is maintained constant to better than 1% in a range of values which are continuously adjustable from 2 to 50 rps. The error signal is given by the voltage to the terminals of a tachometer generator which is compared to an adjustable reference voltage.

- frequency meters, which are composed basically of an electric pulse generator and a counter.

The pulses are produced by the interception of a luminous ray aimed at a photoelectric cell by crenels which are mounted around the circumference of a disk turning with the same speed as the balance motor.

- a sinusoidal current generator with constant intensity and adjustable phase. It is composed of a constant-modulus symmetrical phase converter which was developed at O.N.E.R.A. and several continuous commercially produced transistorized amplifiers. The intensity of the current is maintained constant at better than 1% deviation, no matter what the phase adjustment;

the current which is delivered makes it possible to feed the 10 gage bridges which handle 120 ohms at 16 volts, from peak to peak. The phase adjustment threshold is on the order of 1 milliradian.

The frequency level runs from 2 Hz to 100 Hz. The current direction can be inverted and the phase changed manually and quite rapidly.

- The silicium semi-conductor gages which are presently being put into service and which are 60 times more sensitive than resistance wire gages have made it possible to make some substantial progress with respect to the elements linked to the table mountings. The following example gives an idea of the use of these gages:

It has been possible to increase the sensitivity of the roll dynamometer by seven times and its rigidity by five times through replacing the resistance wire gages which were attached to a support with a cross-shaped section area by semi-conductor gages attached to a support with a rectangular section /8
which encompasses the former area (Figure 4).

The interactions are more important with the gages attached to the sting axis at 45°; however, they are not restrictive since they can be determined quite precisely.

It is to be hoped that in the future these interactions will be diminished through improving the technique of mounting the gages.

Like the dynamometers, the position detectors have been equipped with silicium gages.

- On the other hand, due to the small size of these gages as can be seen from the dimensions:

length 4 mm, width 1 mm, thickness 20 microns, the Department of Physics at O.N.E.R.A. has been able to perfect accelerometers with dimensions which are small enough to permit their being installed inside the mock-ups (4 × 2 × 15 mm).

The measurement threshold is 2.5×10^{-3}g and their natural frequency is greater than one kilocycle.

An example of the installation for these accelerometers is given in Figure 11 and § 4.3.3.1.

4.2 A Comment on the Joints

The use of flexible joints as are currently used in the automobile industry has been adopted for all the balances. As a reminder, it should be pointed out here that they consist of two concentric steel rings (Figure 5) inter-connected by a rubber ring. This piece of equipment, which permits easy correction of alignment errors, is of special interest in damping the shocks at the peak of the test when the motion amplitude reaches its maximum values.

4.3 Development of the Installations

4.3.1 Installation at Chalais-Meudon

At O.N.E.R.A.'s Aerodynamic Research Center at Chalais-Meudon, the measurement of derivatives is conducted along industrial lines in all the wind-tunnels.

It was pointed out earlier (§ 3.3) how this method was extended to cover intermittent wind-tunnels.

The test control organs and the measurement instruments are combined in a measurement station (Plate 8) which is linked up to the wind-tunnels and the laboratory where the mountings are given final adjustment; the communication lines with the transonic wind-tunnel S_3 are up to 800 m long. It was /9
considered of interest to point out this detail due to the very low values of the measurement currents (on the order of 10^{-9} A). This arrangement offers great flexibility in the manner in which the installations function and eliminates the need to move the measurement and control instruments or duplicate them.

4.3.1.1 Example of Mounting on the Subsonic Table

Only one example is given here for the mountings used in recent years. It can be installed either in the large subsonic wind-tunnel S_1 or in the S_2 wind-tunnel. It permits the mock-up to undergo successively oscillations of pitch (Figure 5), yaw (Figures 6 and 7) and roll (Figure 8 and 9).

Plate 12 gives its basic characteristics.

The results obtained with this installation can be compared to flight measurements. Such a comparison is made below in § 5.

4.3.3 The O.N.E.R.A. Transonic and Supersonic S_2 Wind-Tunnel Installations at Modane

Following the adjustments made on the installation at the small wind-tunnels at Chalais-Meudon, two mountings were built to equip this wind-tunnel [4], which has a rectangular experimental stream channel which is 1.87 × 1.75 m and in which the generating pressure p_i and the Mach number M can be controlled continuously at the respective intervals of:

$$0.2 \leq p_i \leq 2 \text{ bars}$$

$$0.2 \leq M \leq 1.3 \qquad \text{and} \qquad 1.5 \leq M \leq 3.2$$

The first mounting sends roll oscillations to the mock-up and the second instills pitch and yaw oscillations.

4.3.3.1 The Diagram for the Roll Balance is given in Figure 8, and its Characteristics are given in Plate 15

Figure 11 shows a view of the dynamometric portion of the sting. This figure shows the two accelerometer pick-ups which permit determination of the parasitic transverse motion of the mock-up resulting from the dynamic deformation of the sting.

Measurement of the direct derivative of the roll moment with respect to the angular velocity p_1, as represented by the coefficient $C_{j_{p1}}$, in general presents no particular difficulty. In fact, the value of the total roll moment, including the mass and aerodynamic effects, does not exceed ten times that of the phase moment with p_1, a condition which still permits measurement of $C_{j_{p1}}$ with an approximation on the order of 10%.

In contrast, determining the coefficient C_{np_1}, which characterizes the /10
crossed derivative of the yaw moment with respect to p_1, demands special precaution.

First, the absolute value of this coefficient is low, in general not exceeding one tenth that of $C_{I_{p_1}}$.

In addition, the yaw moments introduced by the mass and aerodynamic connections cause deformations in the sting which in turn result in other yaw moments. Experience has shown that these moments have components which are in phase with p_1 and which, beyond a certain frequency, substantially exceed the value to be measured.

Theoretical analysis of the phenomenon has shown that the value of the test frequency need simply be held below a specific limit in order for the correction terms to be negligible.

This conclusion has been confirmed through measurements carried out in the supersonic section of the wind-tunnel during testing of the installation's performance with a mock-up of the CONCORDE which was normally used for steady measurements (Figure 12).

4.3.3.2 The Diagram for the Pitch-Yaw Balance is Given in Figure 13

A linear accelerometer of the same type as that used on the roll balance is installed to the right of the dynamometric portion of the sting. It is not indicated in the diagram.

The indications shown by this instrument are taken as the phase origin by the quadrature adjustments discussed in § 3.3 above.

In fact, in the special case of this balance, structural damping of the section of the sting which is not setup could at higher frequencies introduce non-negligible phase displacement between the motion of a mock-up and the signal from the position detector.

5. Comparison with Flight Measurements

Measurements around the three axes have been made on the mounting described in § 4.3.1.1 in the S_1 wind-tunnel, using a motor-driven mock-up of the BREGUET 941 short takeoff and landing aircraft on the scale of 1/7 (Figure 14).

The mass of this mock-up is 60 kg, and its span and length are slightly over 3 meters. It is equipped with four propellers which are 0.6 m in diameter, turning at 2750 rpm and driven by an electric motor installed within the fuselage and a flexible drive similar to that used in the aircraft.

In order to satisfy the laws of mechanical similarity, the operation of the propellers demand low flow velocities within the interval:

$$10 \leq V \leq 15 \text{ m/s}.$$

However, the dynamometers have been shown to be sufficiently sensitive and precise measurements have been achieved in spite of this limitation. /11

Flight tests have been made on this aircraft with the joint cooperation of NASA and the BREGUET company.

Incidentally, the BREGUET company has simulated these tests on an analog computer, adjusting the posted aerodynamic derivatives through success adjustment in order to obtain the best comparison against flight data.

This comparison is made here on the following parameters:

1) Dutch roll.

2) Maximum responses of angular velocities for yaw M_1, roll p_1 and side-slip angle j, to impetus to the rudder.

3) Maximum response of angular velocity of roll p_1 to impetus transmitted to the ailerons.

The values resulting from this study are compared to those measured in the wind-tunnel (Plate 19). Comparison shows that the values of the measured derivatives in the wind-tunnel are in close agreement with the mean values of the derivatives read out on the computer, with the exception of the crossed roll derivatives $C_{l_{j_1}}$ and $C_{l_{r_1}}$.

6. Conclusion

In conclusion, it is possible at this point to furnish designers most of the aerodynamic derivatives necessary for calculation of flight mechanics, with only a slight delay and with the measurements being of a commercial nature.

Study of these derivatives with respect to acceleration has just gotten underway at O.N.E.R.A. and was patterned after the setup used at the CORNELL Laboratory in the U.S.A., although the results obtained are still too modest to be presented here.

Thus, we are beginning to obtain encouraging comparisons between flight results on aircraft studied by the unsteady methods in wind-tunnels.

REFERENCES /12

1. Scherer, M.: Mesure des derivees aerodynamiques en soufflerie et en vol [Measurement of Aerodynamic Derivatives in Wind-Tunnels and in Flight], AGARD Report 346, April 1961.
2. Vaucheret, X.: Stabilite dynamique sur maquette d'avion par la methode des oscillations libres [Dynamic Stability in Aircraft Mock-ups by the Method of Free Oscillations], O.N.E.R.A. preprint No. 390 AGARD, CAMBRIDGE 1966.
3. Mathot, F.: Methode de mesure des derivees aerodynamiques en soufflerie hypersonique a rafales [A Method for Measuring Aerodynamic Derivatives in an Intermittent Hypersonic Wind-tunnel], To appear in Recherche Aerospatiale, No. 114, 1966.
4. Statler, D.C., Tufts, O.B., and Mirtreiter, W.J.: [A New Capability for Measuring Dynamic Air Loads in a Wind-Tunnel], A.I.A.A. Paper, New York, January 1966.
5. Souffleries O.N.E.R.A. [O.N.E.R.A. Wind-Tunnels], O.N.E.R.A. Publication, 1965.

LISTS OF PLATES

Standard or reference trihedral Gx_1, y_1, z_1 is fastened to the moving body.	FORCES		
	Longitudinal force	Transverse force	Normal force
Forces and moments	$-R_{x_1} = \frac{\rho}{2} V^2 S C_{x_1}$	$-R_{y_1} = \frac{\rho}{2} V^2 S C_{y_1}$	$-R_{z_1} = \frac{\rho}{2} V^2 S C_{z_1}$
Dimensionless coefficients	$C_{x_1} = -\frac{R_{x_1}}{\frac{\rho}{2} V^2 S}$	$C_{y_1} = -\frac{R_{y_1}}{\frac{\rho}{2} V^2 S}$	$C_{z_1} = -\frac{R_{z_1}}{\frac{\rho}{2} V^2 S}$
Velocities	Translation velocities of center of gravity		
	u_1	v_1	w_1

	DIMENSIONLESS COEFFICIENTS		
Functions / Variables	R_{x_1} Longitudinal force	R_{y_1} Transverse force	R_{z_1} Normal force
i Angle of incidence	$C_{xi_1} = -\frac{1}{\frac{\rho}{2} V^2 S} \frac{\partial R_{x_1}}{\partial i}$		$C_{zi_1} = -\frac{1}{\frac{\rho}{2} V^2 S} \frac{\partial R_{z_1}}{\partial i}$
j Side-slip angle	$C_{xj_1} = -\frac{1}{\frac{\rho}{2} V^2 S} \frac{\partial R_{x_1}}{\partial j}$	$C_{yj_1} = -\frac{1}{\frac{\rho}{2} V^2 S} \frac{\partial R_{y_1}}{\partial j}$	
α_1 Aileron extension angle	$C_{x\alpha_1} = -\frac{1}{\frac{\rho}{2} V^2 S} \frac{\partial R_{x_1}}{\partial \alpha_1}$	$C_{y\alpha_1} = -\frac{1}{\frac{\rho}{2} V^2 S} \frac{\partial R_{y_1}}{\partial \alpha_1}$	
β_1 Angle of elevator extension	$C_{x\beta_1} = -\frac{1}{\frac{\rho}{2} V^2 S} \frac{\partial R_{x_1}}{\partial \beta_1}$		$C_{z\beta_1} = -\frac{1}{\frac{\rho}{2} V^2 S} \frac{\partial R_{z_1}}{\partial \beta_1}$
δ_1 Angle of rudder extension	$C_{x\delta_1} = -\frac{1}{\frac{\rho}{2} V^2 S} \frac{\partial R_{x_1}}{\partial \delta_1}$	$C_{y\delta_1} = -\frac{1}{\frac{\rho}{2} V^2 S} \frac{\partial R_{y_1}}{\partial \delta_1}$	
p_1 Roll angular velocity		$C_{yp_1} = -\frac{1}{\frac{\rho}{2} V^2 S} \frac{\partial R_{y_1}}{\partial p_1 \frac{\ell}{V}}$	
q_1 Pitch angular velocity			$C_{zq_1} = -\frac{1}{\frac{\rho}{2} V^2 S} \frac{\partial R_{z_1}}{\partial q_1 \frac{\ell}{V}}$
r_1 Yaw angular velocity		$C_{yr_1} = -\frac{1}{\frac{\rho}{2} V^2 S} \frac{\partial R_{y_1}}{\partial r_1 \frac{\ell}{V}}$	

MOMENTS		
Roll	Pitch	Yaw
$L_1 = \frac{\rho}{2} V^2 S l C_{l_1}$	$M_1 = \frac{\rho}{2} V^2 S l C_{m_1}$	$N_1 = \frac{\rho}{2} V^2 S l C_{n_1}$
$C_{l_1} = \frac{L_1}{\frac{\rho}{2} V^2 S l}$	$C_{m_1} = \frac{M_1}{\frac{\rho}{2} V^2 S l}$	$C_{n_1} = \frac{N_1}{\frac{\rho}{2} V^2 S l}$
Angular velocities		
p_1	q_1	r_1
OF AERODYNAMIC DERIVATIVES		
L_1 Roll moment	M_1 Pitch moment	N_1 Yaw moment
	$C_{mi_1} = \frac{1}{\frac{\rho}{2} V^2 S l} \frac{\partial M_1}{\partial i}$	
$C_{lj_1} = \frac{1}{\frac{\rho}{2} V^2 S l} \frac{\partial L_1}{\partial j}$		$C_{nj_1} = \frac{1}{\frac{\rho}{2} V^2 S l} \frac{\partial N_1}{\partial j}$
$C_{l\alpha_1} = \frac{1}{\frac{\rho}{2} V^2 S l} \frac{\partial L_1}{\partial \alpha_1}$		$C_{n\alpha_1} = \frac{1}{\frac{\rho}{2} V^2 S l} \frac{\partial N_1}{\partial \alpha_1}$
	$C_{m\beta_1} = \frac{1}{\frac{\rho}{2} V^2 S l} \frac{\partial M_1}{\partial \beta_1}$	
$C_{l\delta_1} = \frac{1}{\frac{\rho}{2} V^2 S l} \frac{\partial L_1}{\partial \delta_1}$		$C_{n\delta_1} = \frac{1}{\frac{\rho}{2} V^2 S l} \frac{\partial N_1}{\partial \delta_1}$
$C_{lp_1} = \frac{1}{\frac{\rho}{2} V^2 S l} \frac{\partial L_1}{\partial p_1 \frac{l}{V}}$		$C_{np_1} = \frac{1}{\frac{\rho}{2} V^2 S l} \frac{\partial N_1}{\partial p_1 \frac{l}{V}}$
	$C_{mq_1} = \frac{1}{\frac{\rho}{2} V^2 S l} \frac{\partial M_1}{\partial q_1 \frac{l}{V}}$	
$C_{lr_1} = \frac{1}{\frac{\rho}{2} V^2 S l} \frac{\partial L_1}{\partial r_1 \frac{l}{V}}$		$C_{nr_1} = \frac{1}{\frac{\rho}{2} V^2 S l} \frac{\partial N_1}{\partial r_1 \frac{l}{V}}$

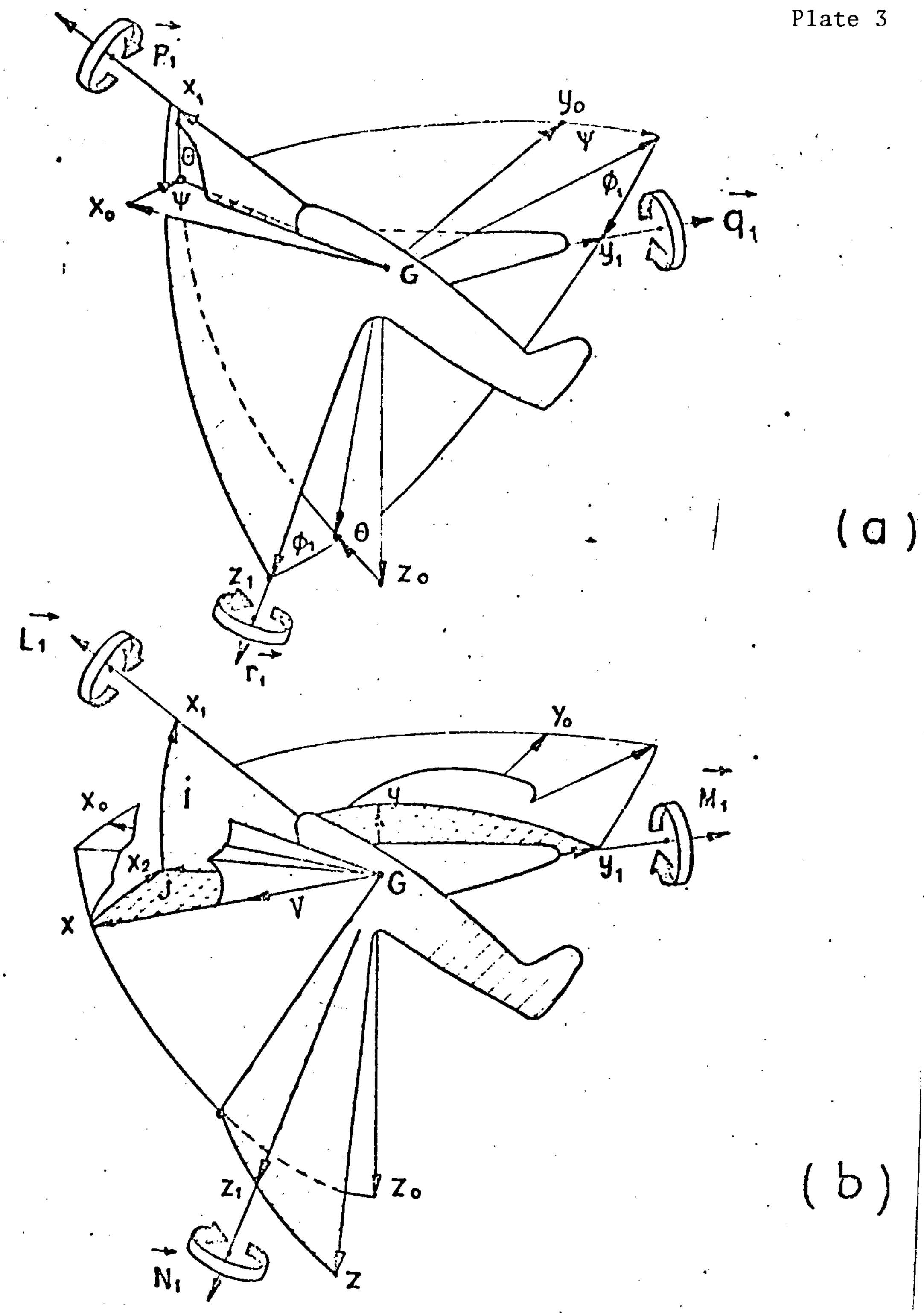

Figure 1. Coordinate Axes Defining the Position of the Aircraft in Space (a) and on Trajectory (b).

Caption to Figure 1

G $x_0y_0z_0$ Galilean coordinate axis, G z_0 being the vertical;

G $x_1y_1z_1$ Aircraft coordinate axis, G x_1z_1 being the plane symmetry;

The angles represented are positive, the curve arrows indicate the positive direction of the components of angular velocity (a) and of aerodynamic moment (b).

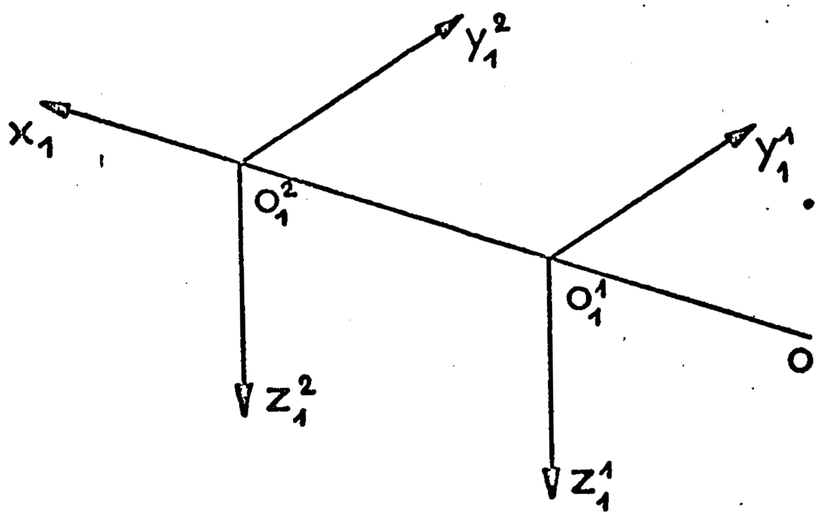

Figure 2. Sting Coordinate Axes

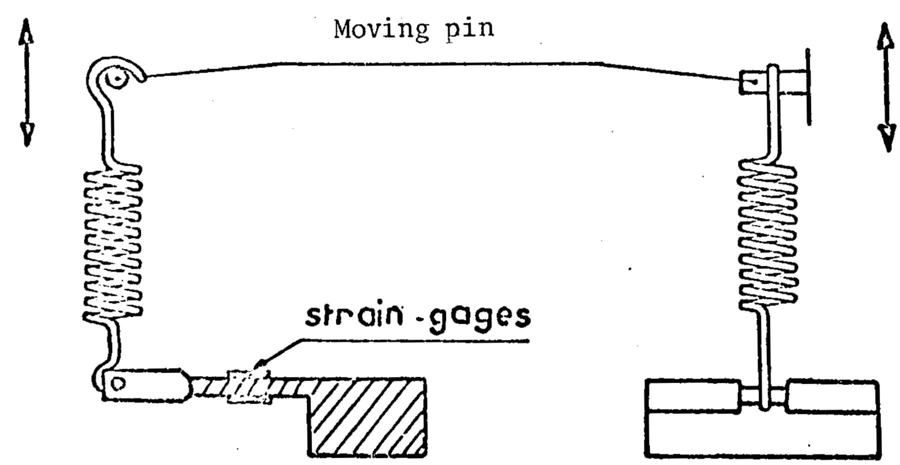

Figure 3. Position Detector

Plate 5

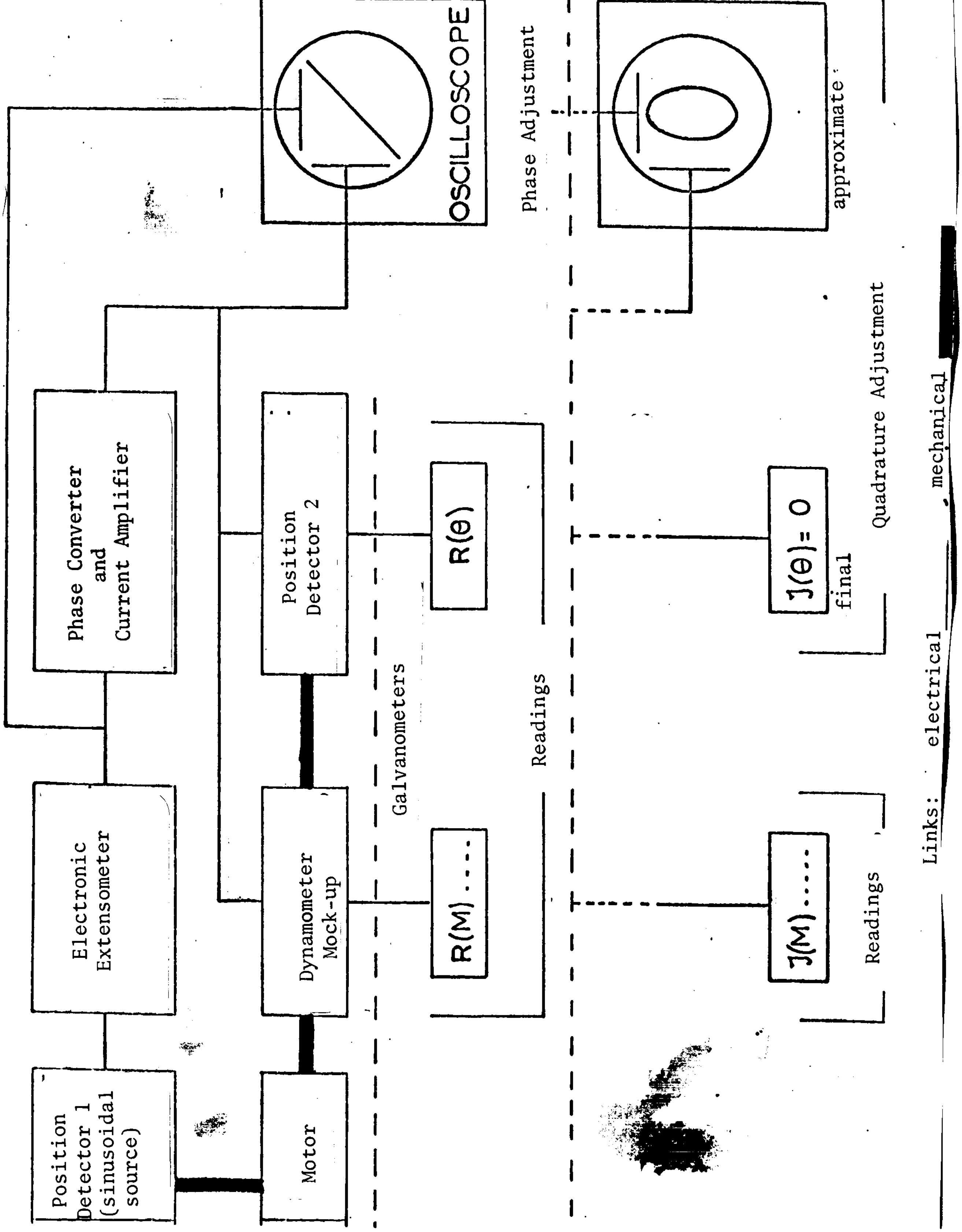

Position Detector 1 (sinusoidal source)
Electronic Extensometer
Phase Converter and Current Amplifier
Motor
Dynamometer Mock-up
Position Detector 2
OSCILLOSCOPE
Galvanometers
R(M) . . . .
R(θ)
Readings
Phase Adjustment
approximate
J(M) . . . .
J(θ) = 0
final
Readings
Quadrature Adjustment
Links: electrical mechanical

Plate 6

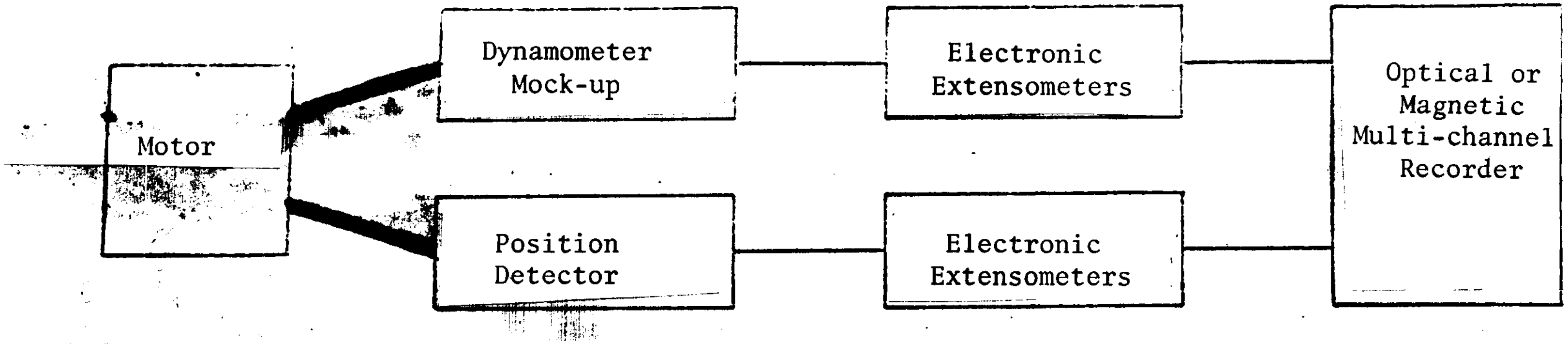

1 - Wind-tunnel Measurement Setup

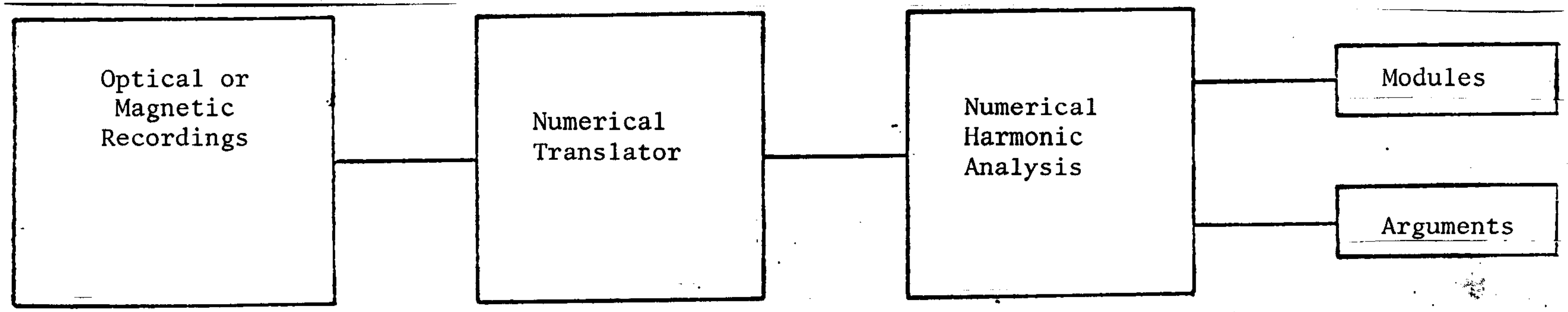

2 - Numerical Harmonic Reading and Analysis

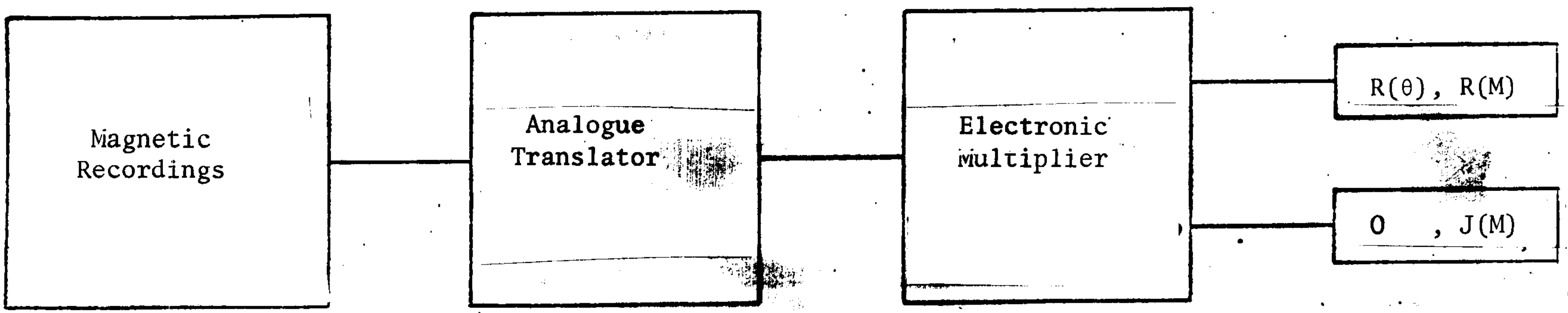

3 - Harmonic Analogue Reading and Analysis

Plate 7

ROLL DYNAMOMETER

Comparison in sensitivity and flexibility

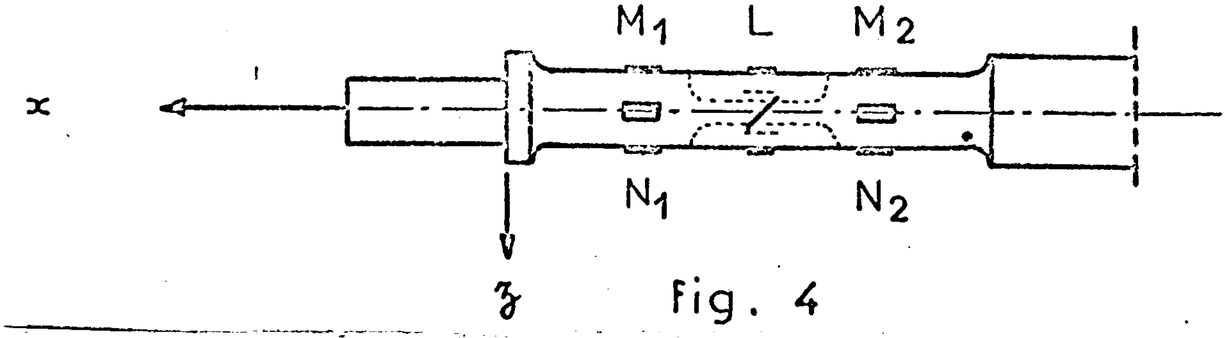

Fig. 4

Strain detector	Semi-conductor	Resistance wire	
Section	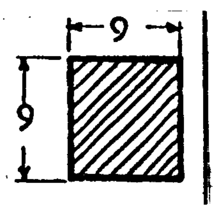	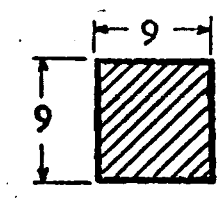	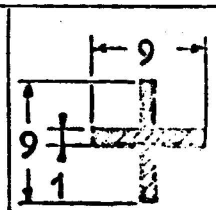
Roll response in 10^{-6} $\Delta R/R$ for L = 9.81 m.N	180,000	3,000	25,000
Interactions in % of L due to M	3%	None unmeasured	<0.1%
N	1%		
R_y	0.1%		
R_z	0.4%		
Flexibility $\Delta\Phi/_{\Delta L}$ in r/mN	0.0031	0.0031	0.016

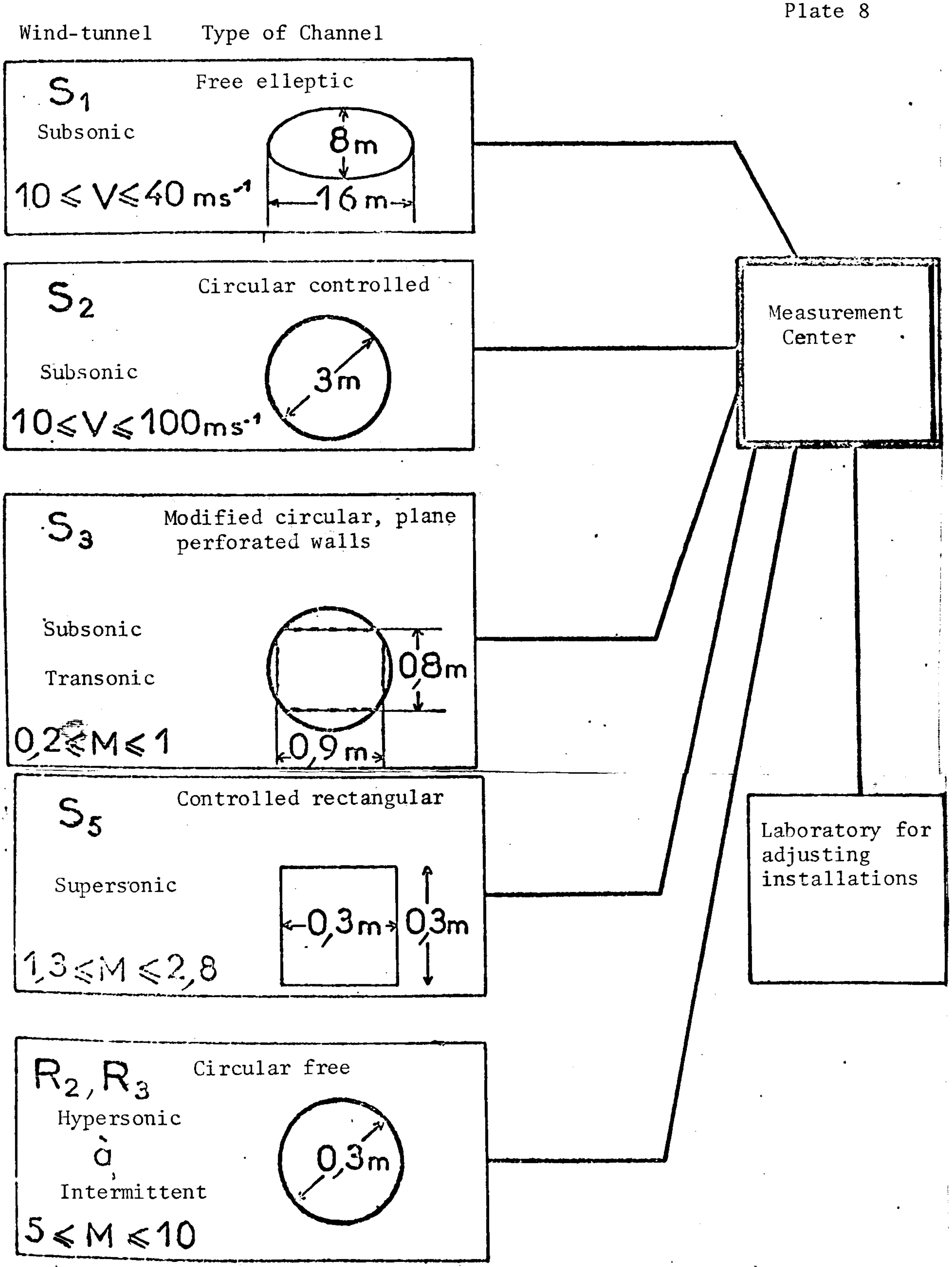
Wind-tunnel
Type of Channel
S1
Subsonic
Free elleptic
8m
16 m
10 ≤ V ≤ 40 ms-1
S2
Subsonic
Circular controlled
3m
10 ≤ V ≤ 100 ms-1
S3
Subsonic
Transonic
Modified circular, plane perforated walls
0,8m
0,9 m
0,2 ≤ M ≤ 1
S5
Supersonic
Controlled rectangular
0,3m
0,3m
1,3 ≤ M ≤ 2,8
R2, R3
Hypersonic
à
Intermittent
Circular free
0,3m
5 ≤ M ≤ 10
Measurement Center
Laboratory for adjusting installations

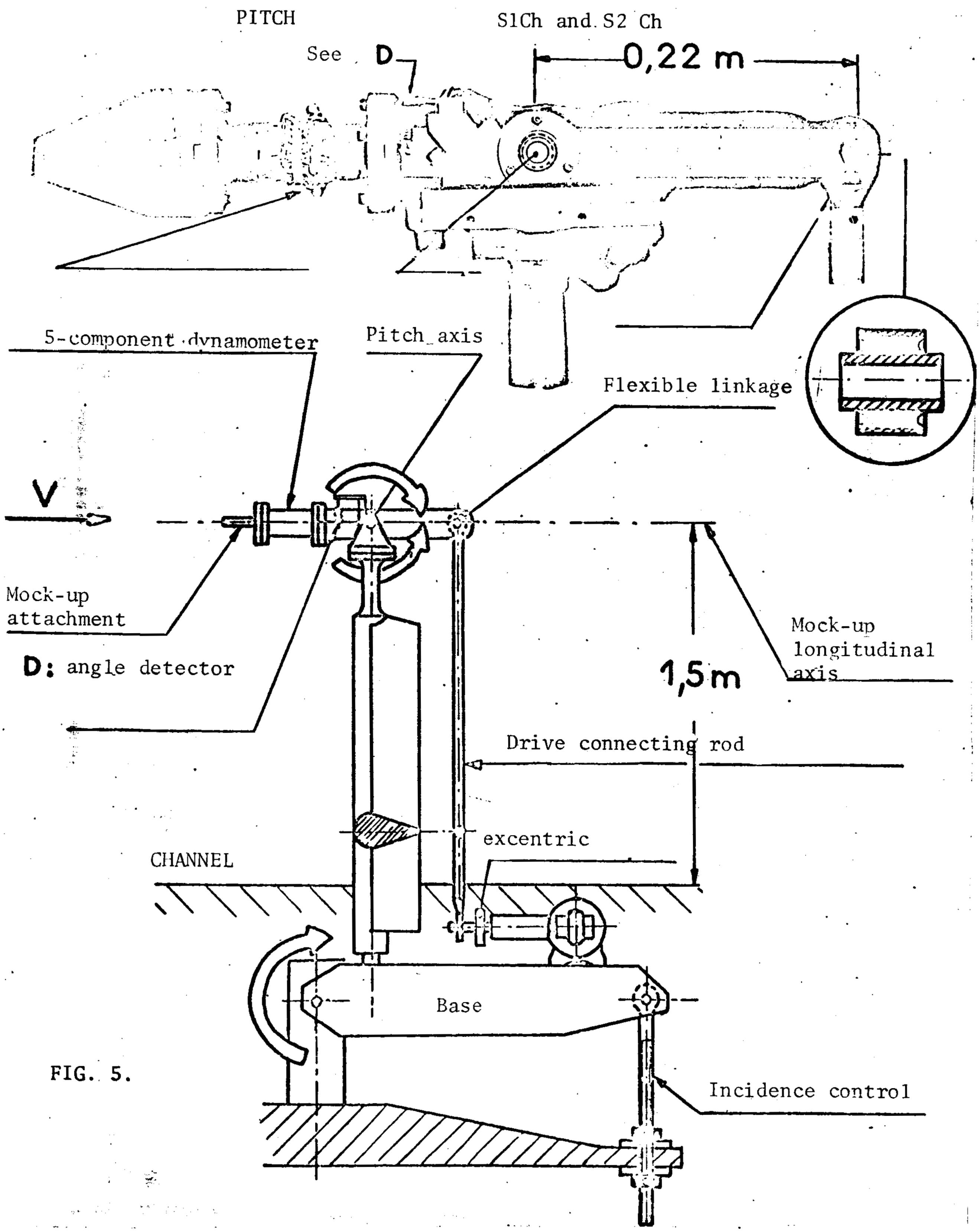
PITCH
S1Ch and S2 Ch
See D
0,22 m
5-component dynamometer
Pitch axis
Flexible linkage
V
Mock-up attachment
D: angle detector
1,5 m
Mock-up longitudinal axis
Drive connecting rod
excentric
CHANNEL
Base
Incidence control

FIG. 5.

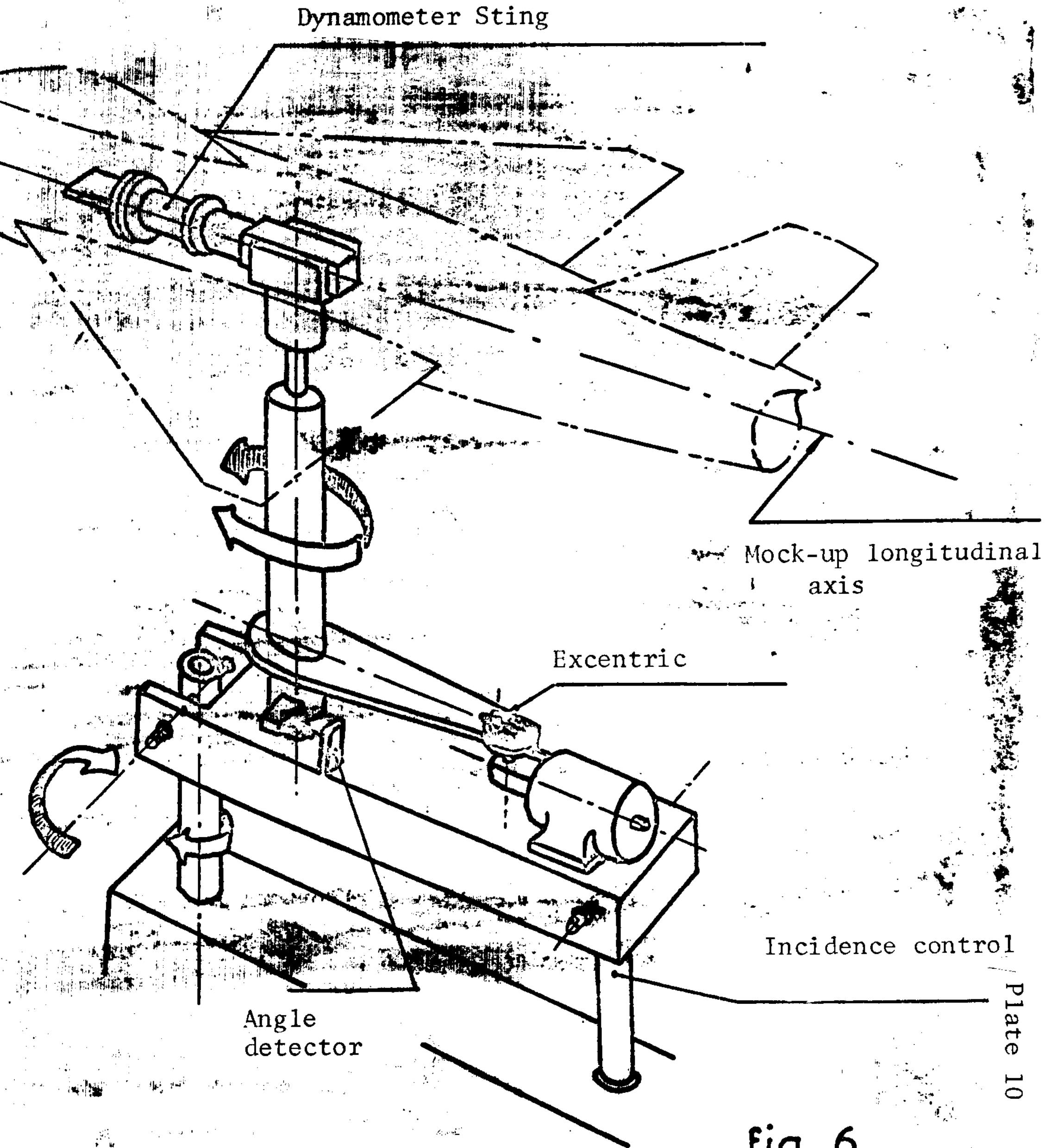
Dynamometer Sting
Mock-up longitudinal axis
Excentric
Incidence control
Angle detector

fig. 6

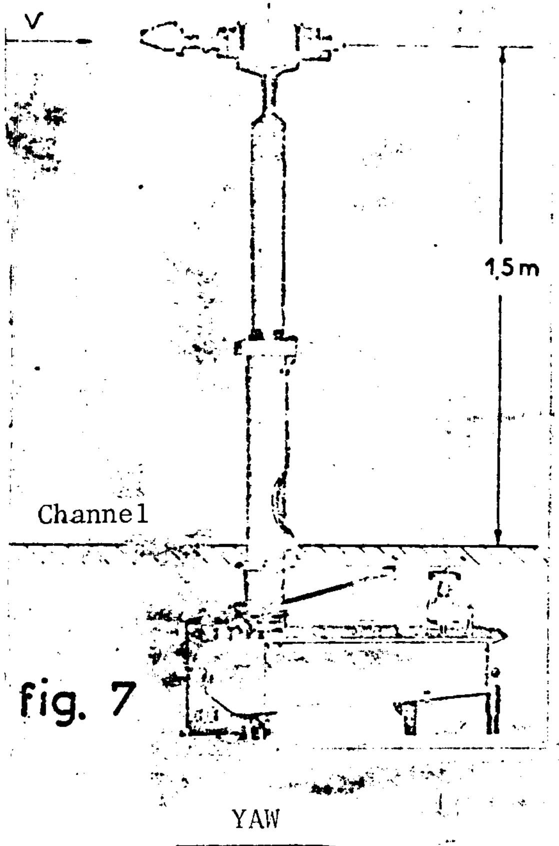
V
1,5 m
Channel
YAW

fig. 7

Plate 11

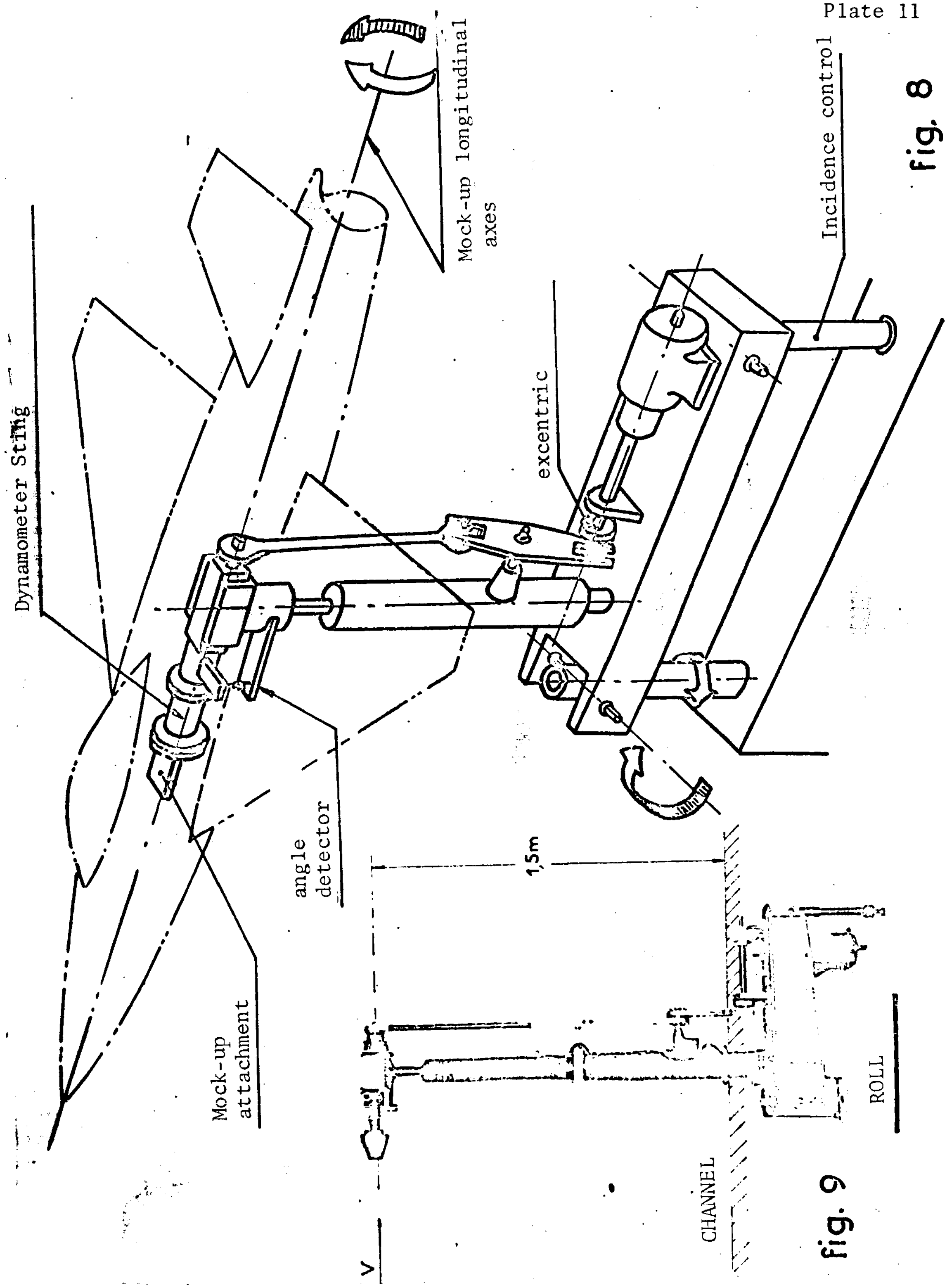

fig. 8

fig. 9

THE CHALAIS-MEUDON S_1 AND S_2 BALANCE.

Amplitudes	θ, ψ_1, ϕ_1 .	± 1 à ± 3 degrees
Mean incidence		$0 \leq i \leq 30$ degrees
Mean side-slip		$-12 \leq i \leq 12$ degrees
Frequency		$1 \leq f \leq 2$ Hz
5-component moment dynamometer		$L_1 \& \begin{cases} M_1^1 \quad N_1^1 & \text{leading} \\ M_1^2 \quad N_1^2 & \text{trailing} \end{cases}$
Distance between leading and trailing axes		6.3 mm
Maximum amplitudes of moments		$\pm$ 100 Nm
Measurement threshold		0,04 Nm
Maximum mock-up mass		60 Kg
Size of balance head		cylinder ∅ 15 cm length 60 cm

Plate 13

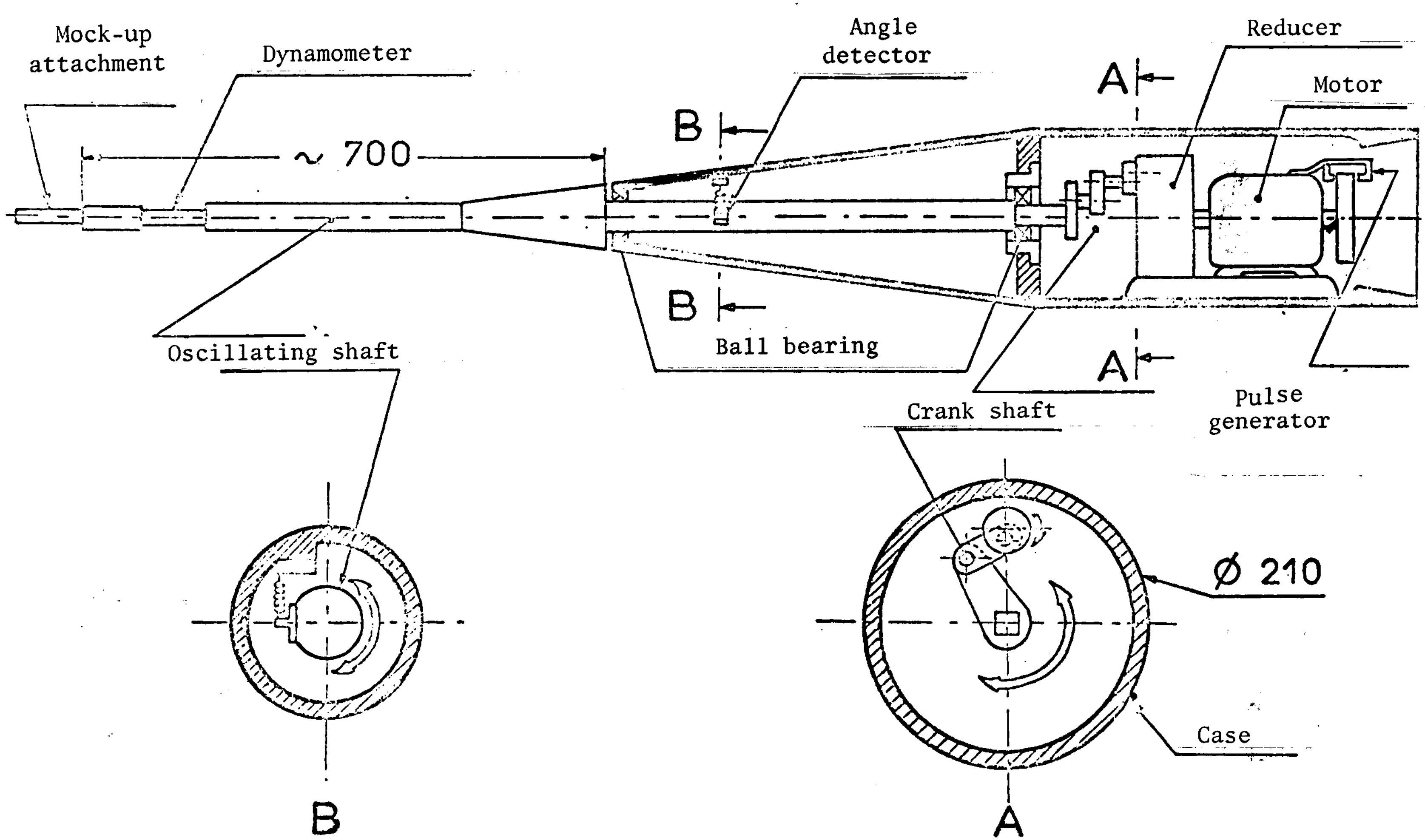

Figure 10. S2 Modane Roll Balance

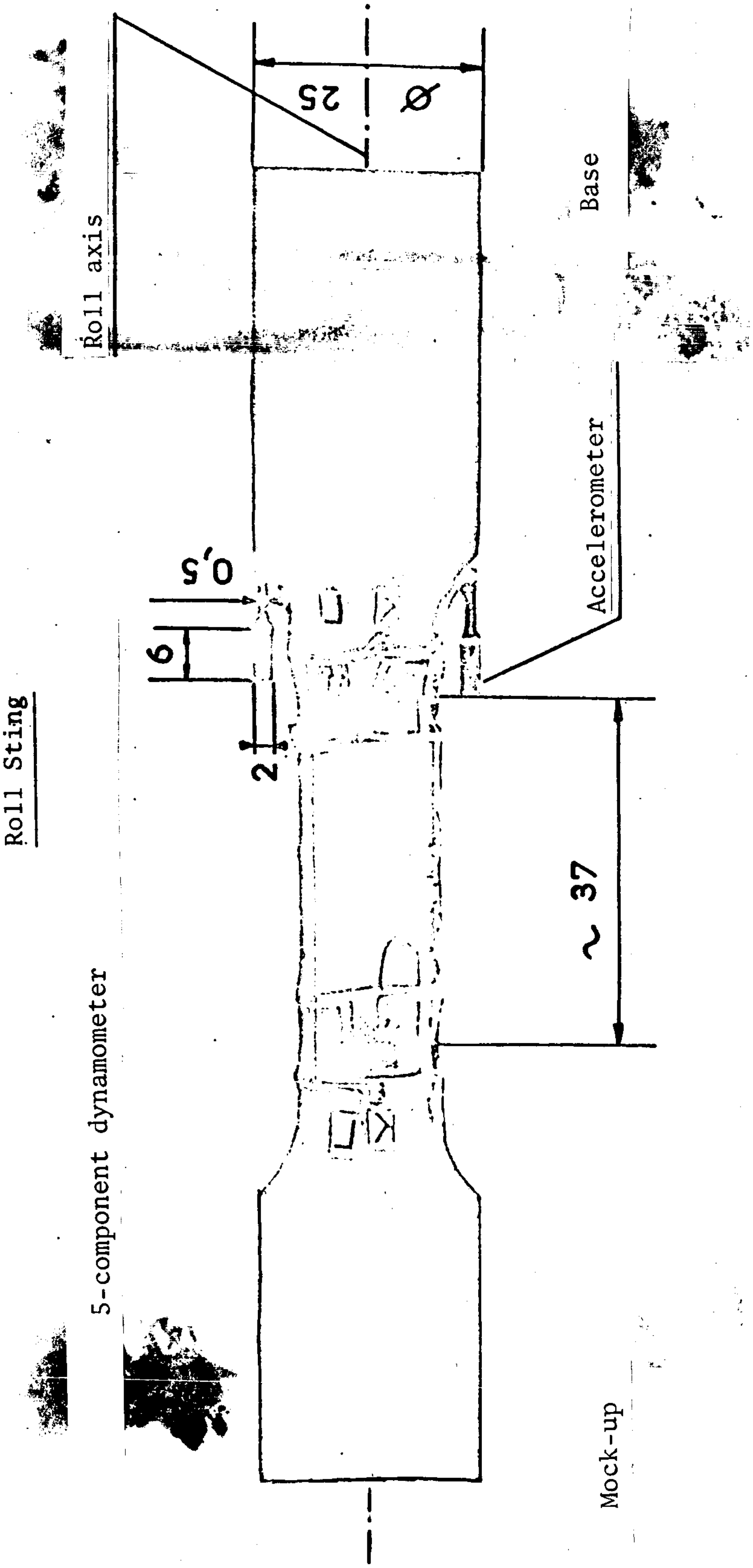
Roll Sting
Roll axis
5-component dynamometer
Base
Accelerometer
Mock-up
25
⌀
0,5
6
2
~ 37

fig. 11

MODAN S_2 ROLL BALANCE

Roll angle amplitude Φ	± 3 degrees
Frequency	$5 \leq f \leq 10$ Hz
5-component moment dynamometer	L_1 & $\begin{cases} M_1^1 \quad N_1^2 \text{ leading} \\ M_1^2 \quad N_1^2 \text{ trailing} \end{cases}$
Distance between leading and trailing axes	34 mm
Maximum amplitude of moments	30 Nm
Measurement threshold	0.01 Nm
Transverse accelerometer; measurement threshold	0.0025 g
Dimensions of cylinder wall for dynamometer sting	$\begin{cases} \text{diameter } 25 \text{ cm} \\ \text{length } 60 \text{ cm} \end{cases}$
Mock-up mass	6 Kg

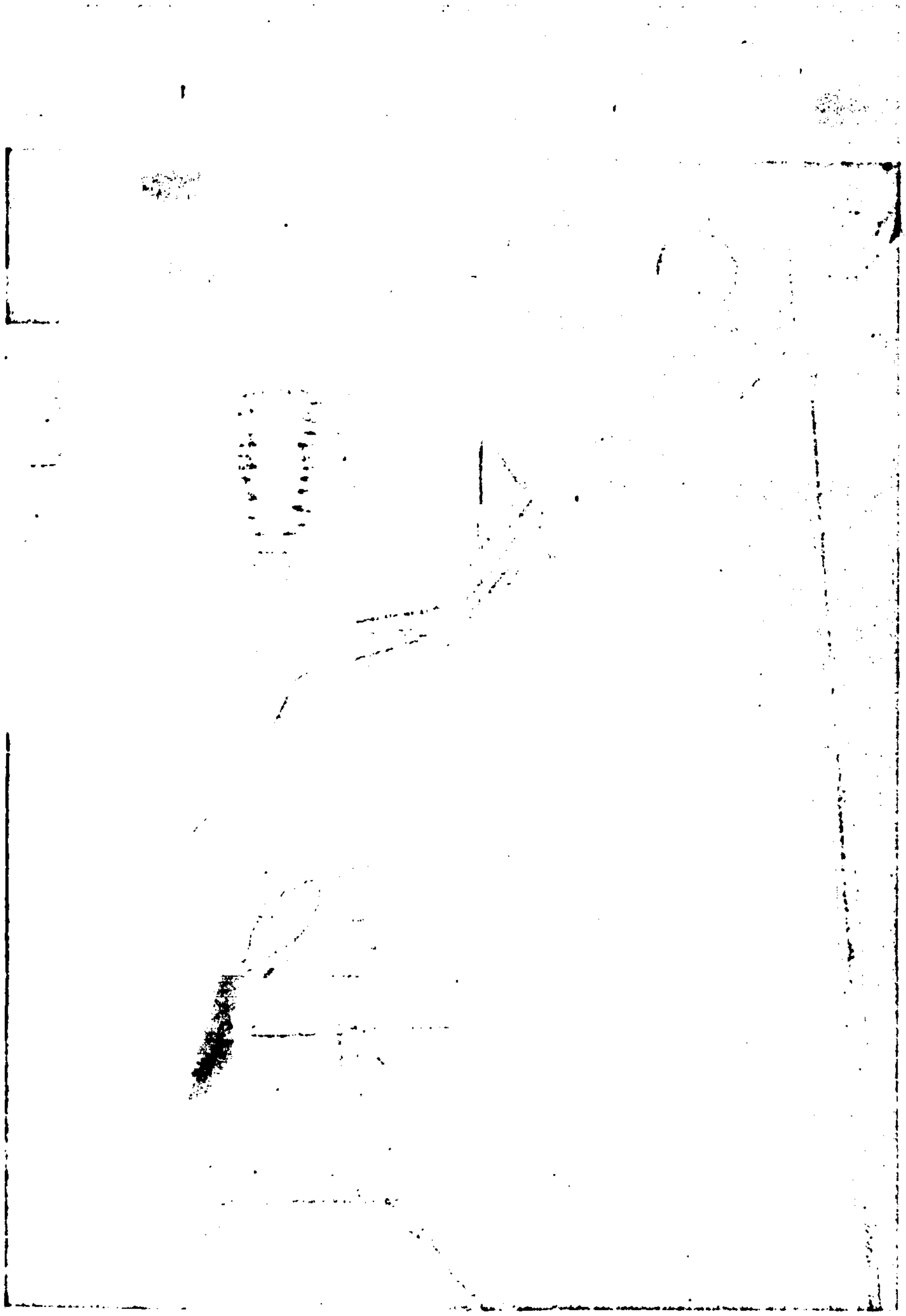

fig. 12

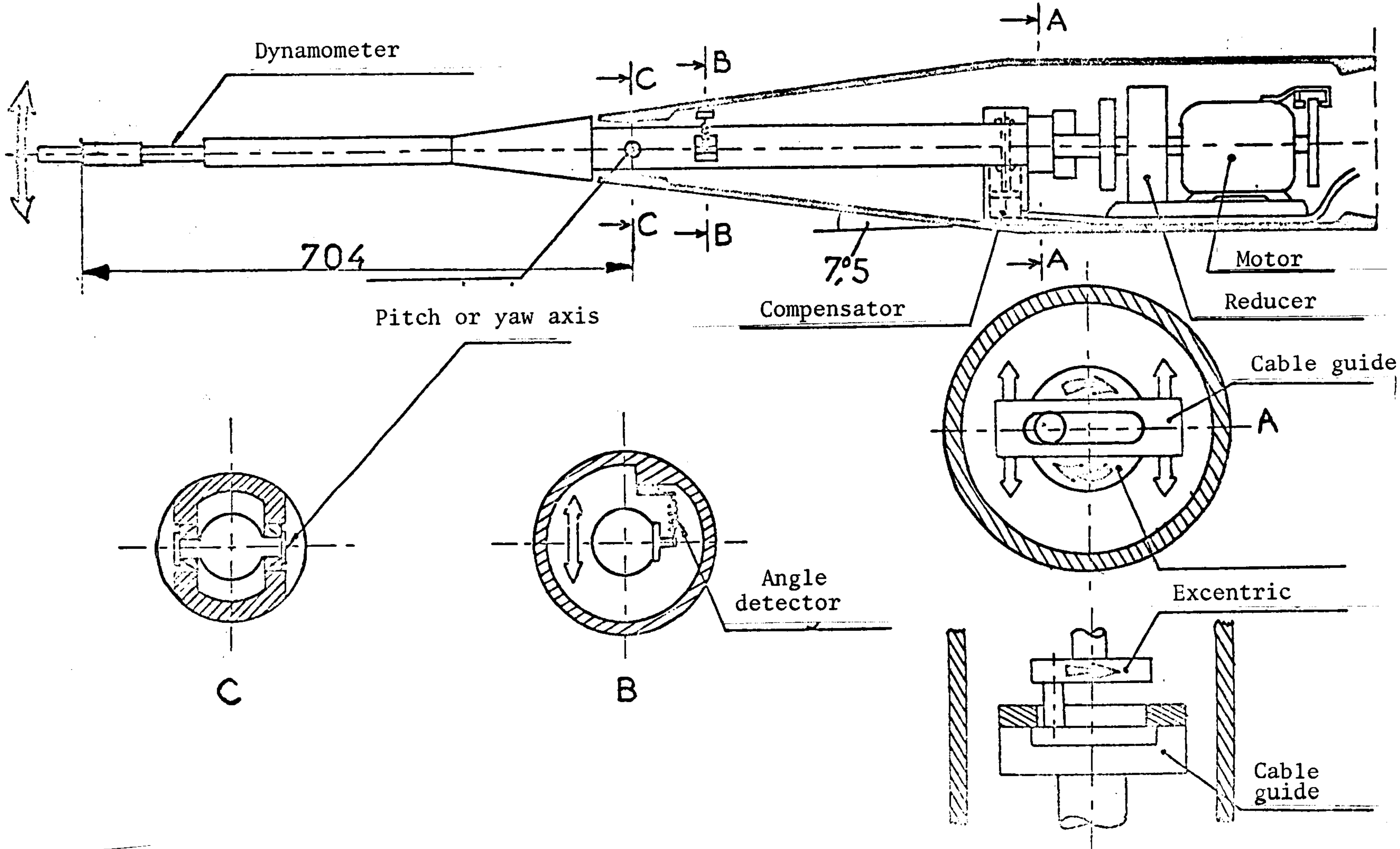

Figure 13. Pitch-Yaw Balance for MA S2

BREGUET 941

Landing Configuration

1) Comparison of results from flight and analogue computer

	SYMBOL	FLIGHT	COMPUTER (1)	(2)
Dutch roll	time in seconds	8.1	7.4	8.7
Responses to one step on rudder				
Angular velocity of maximum yaw	$r_1 (rs^{-1})$	-0.16	-0.2	-0.17
Angular velocity of maximum roll	p_1(")	-0.09	-0.1	-0.12
Side-slip angle	j dg	27.5°	25°	25°
Response to one step on ailerons				
Angular velocity of maximum roll	$p_1 (rs^{-1})$	0.4	0.45	0.41

2) Comparison of computer and wind-tunnel

Coefficients		Clp_1	Cnr_1	Cnp_1	Clr_1	Clj_1	Cnj_1	Gyration radii (m) r_{xx}	r_{zz}
Analogue computer	1	-8.5	-8	0	6	0.6	-1.5	4	5.2
	2	-10	-15	-2.4	2	0.5	-1.6	4.2	5.9
Wind-tunnel		-11.5	-12	-1.2	10	1	-1.5		

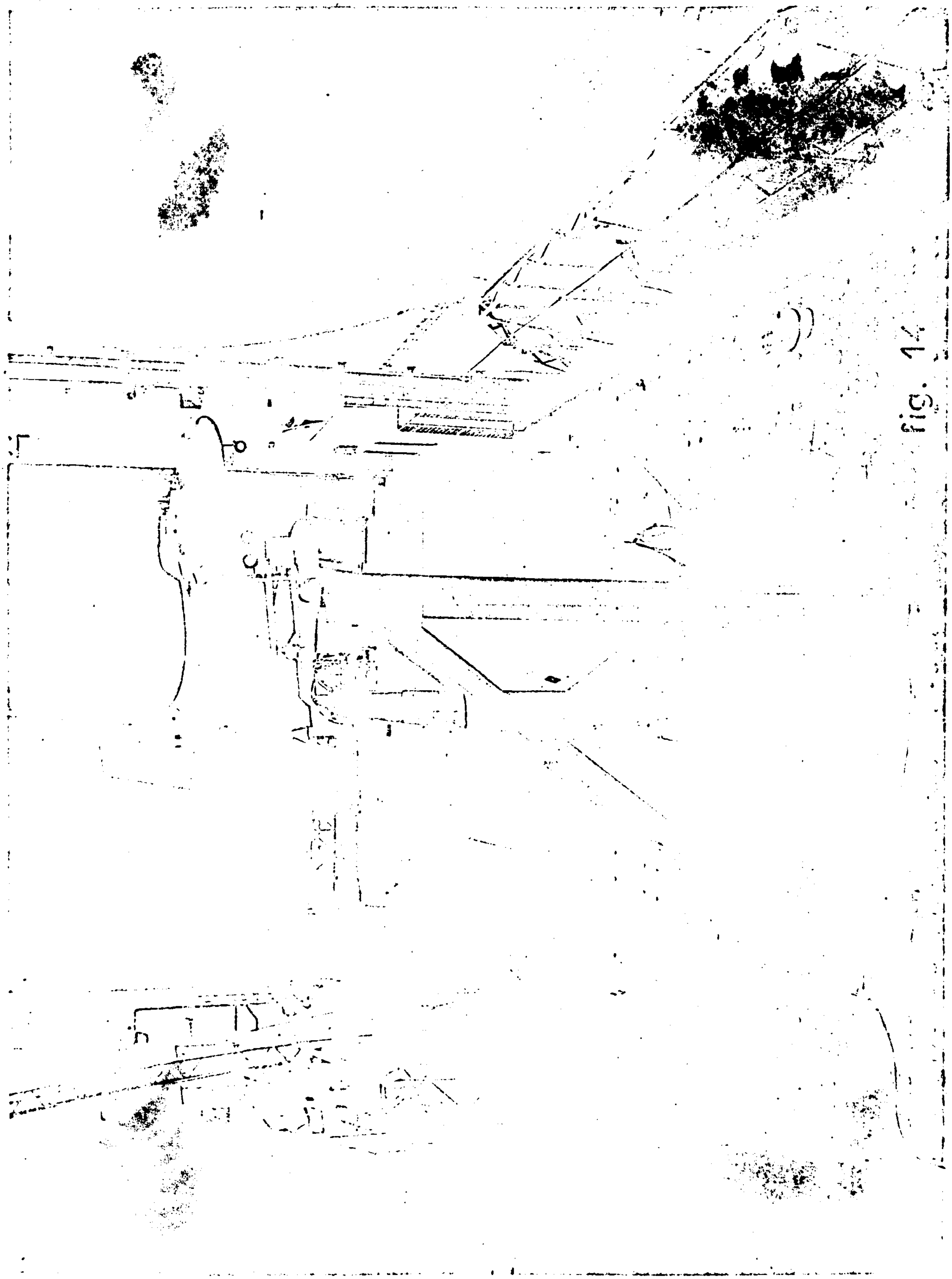

fig. 14